

# Effects Of MHD and Heat Generation/Absorption on UCM Fluid Across A Porous Stretching Surface

Patil Priyanka<sup>1</sup>, Jagadish V. Tawade<sup>2\*</sup>, Pradeep G. Janthe<sup>3</sup>, Suresh Biradar<sup>4</sup>

Submitted: 06/05/2024 Revised: 19/06/2024 Accepted: 26/06/2024

**Abstract:** In the current study, the influences of the numerical study of thermal conductivity in the presence of non-uniform heat sources or sinks and MHD (magnetic field) motivate us to examine the impact of thermal conductivity characteristics of Maxwell fluid over a porous stretching sheet. We delve into various parameter effects through graphical representations. The presence of a transverse magnetic field in an incompressible, electrically conducting fluid causes the velocity field to decrease, causing the temperature field to rise. The results reveal that temperature rises for positive values of the heat source/sink parameters and falls for negative values. Therefore, non-uniform heat sinks are preferable for cooling purposes.

**Keywords:** *Stretching surface, UCM fluid, Magnetic field, heat generation/absorption, porous medium.*

## 1 Introduction

Studying flow induced by a stretching surface in a still fluid and subsequent heat transfer is crucial for various technological applications, such as plastic sheet extrusion, wire production, papermaking, crystal growth, and glass blowing. These processes require bringing molten liquid into a cooling system and occasionally stretching it, as in polymer extrusion, to cool it. Achieving the desired fluid properties in such processes is based on cooling rate and stretching rate. Selecting the right cooling liquid is essential as it directly affects the cooling rate, and optimal stretching must be maintained to avoid unwanted property changes. Therefore, The major goal of this study is to have a thorough comprehension of flow heat transfer characteristics.

In the realm of numerous applications similar to the process of polymer extrusion, Crane [1] pioneered the analytical examination of boundary layer flow caused by a stretching sheet. He assumed that the sheet's velocity varied linearly with distance from slit. In the context of the Navier-Stokes equations, Crane's solution for the flow caused by a stretched sheet is an important illustration of an exact solution, and its singularity has long been proved. Many authors have since explored the presence and uniqueness of solutions for stretching sheet-induced flow, as documented by Rajagopal and McLeod [2] and Troy et

<sup>1,2,3</sup>Department of Mathematics, Vishwakarma University, Pune-411048, Maharashtra, INDIA,

patilpiyu717@gmail.com<sup>1</sup>

jagadish.tawade@vupune.ac.in<sup>2</sup>

pradeepjanthe@gmail.com<sup>3</sup>

<sup>4</sup>Department of Mathematics, Sharanbasva University, Kalaburagi-585103, India.

sureshmaths123@gmail.com<sup>4</sup>

\* Corresponding author: Jagadish V. Tawade

al [3]. McLeod and Rajagopal's analytical investigation sheds light on the treatment of infinity when solving ordinary differential equations in bounded domains.

More recently, several researchers have extended Crane's work to encompass Newtonian and non-Newtonian boundary layer flows under different physical conditions. When examining heat transfer from an isothermal stretched sheet, Gupta and Gupta [4] took suction/blowing effects into account. Gupta and Gupta's study was developed by Chen and Char [5] to handle non-isothermal stretching sheets with suction and blowing. Using the power law fluctuation of surface temperature, Grubka, and Bobba [6] conducted heat transfer investigations, while Chiam [7] examined magnetohydrodynamic heat transfer from a non-isothermal stretched sheet.

The impact of the heat source/sink phenomenon is a crucial aspect deserving careful attention, as it wields a significant effect on the heat transfer characteristics within exothermic processes. Numerous researchers have explored heat transfer phenomena by examining either a constant heat source/sink or one that varies with temperature, as seen in the works of Rollins and Vajravelu [8]. Furthermore Emad [9] expanded on this by considering the impact of a non-uniform heat source/sink, which varies in both space and temperature, on heat transfer.

Non-Newtonian 2<sup>nd</sup>-grade fluid proves inadequate in yielding meaningful outcomes when dealing with highly elastic fluids like polymer melts, especially at high Deborah numbers (See Hayat et al. [10, 11]). Consequently, the importance of the findings presented in the aforementioned studies is somewhat constrained, particularly in the context of the polymer industry. It is

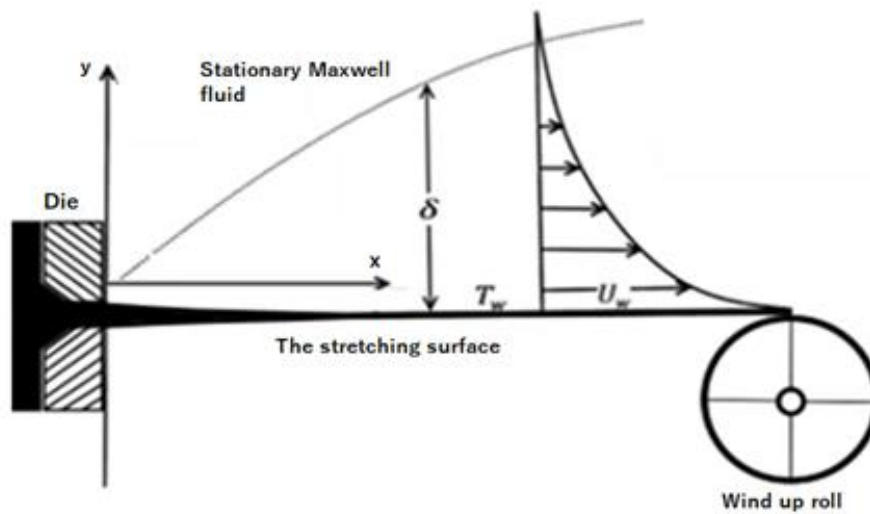
essential to use more realistic viscoelastic fluid models, such as the Upper-Convected Maxwell model or the Oldroyd-B model, in the study to give the theoretical conclusions industrial significance. As mentioned by Sadeghy et al. [12], and Hayat et al. [13] These 2 fluid models were recently applied to examine the viscoelastic fluids flow through both stretching” and non-stretched surfaces. However, heat transfer effects were not taken into account.

Several researchers like Sadeghy[14], Alizadeh-Pahlavan et al. [15, 18], Renardy[16], Rao and Rajagopal [17], Aliakbar et al. [19,20],etc..., have all explored the UCM fluids using the various analytical and numerical methods with or without considering the heat transfer effects.

However, the influence of thermal conductivity in the incidence of non-uniform heat sources or sinks motivates us to examine the impact of thermal conductivity features of Maxwell fluid across a porous stretching sheet. We delve into various parameter effects through graphical representations.

## 2 Mathematical Formulation

The flow is caused due to “stretching of a porous sheet”, that drags from a thin slit. Two forces of equal magnitude but in opposite directions are applied to the sheet in a way that stretches the wall while keeping its starting point unmovable.



Schematic diagram of the flow problem

The equations governing the flow problem (Refs. Renardy[12],Sadeghy et.al[16], Alizadeh-Pahlavan and Sadeghy[15]) are as mentioned below.

$$u_x + u_y = 0 \quad (1)$$

$$uu_x + vu_y + \lambda[u^2u_{xx} + v^2u_{yy} + 2uvu_{xy}] = vu_{yy} - \frac{\sigma B_0^2}{\rho}u - \frac{v}{k'}u, \quad (2)$$

$$uT_x + vT_y = \frac{k}{\rho C_p}T_{yy} + \frac{q'''}{\rho C_p} + \frac{\mu}{\rho C_p}u_y^2 \quad (3)$$

where “ $u$  and  $v$ ” denote the velocity components along  $x$  and  $y$  directions respectively,  $T$  denotes the temperature of the fluid,  $\sigma$  presents the density,  $\nu$  represents the kinematic viscosity,  $k'$  denotes the porosity parameter,  $C_p$  signifies the specific heat at constant pressure,  $k$  indicates the thermal conductivity of the liquid far away from the sheet,  $B_0$ , denotes the strength of the magnetic field,  $\nu$  represents the inematic viscosity of the fluid and  $\lambda$  denotes the relaxation time Parameter of the fluid. The model of the

non-uniform heat source/sink,  $q'''$ , is as follows: (see Chiam[7])

$$q''' = \frac{ku_w(x)}{xv} [A * (T_s - T_0)f' + (T - T_0)B *], \quad (4)$$

where the coefficients  $A^*$  and  $B^*$  represent the space-dependent heat source/sink and temperature-dependent properties, respectively. Here, we make a note that the scenario in which,  $A^* > 0, B^* > 0$  corresponds to the formation of heat on the inside of the system, and that is the case in which,  $A^* < 0, B^* < 0$  corresponds to the absorption of heat on the inside of the system.

The boundary conditions are,  $u = bx, v = 0, T = T_w = T_\infty + A\left(\frac{x}{l}\right)^2$  PSTC case

$$-KT_y = Q_w = D\left(\frac{x}{l}\right)^2 \text{ PHF Case at } y = 0$$

$$u \rightarrow 0, u_y \rightarrow 0, T \rightarrow T_\infty, \text{ as } y \rightarrow \infty \quad (5)$$

Here  $A$  and  $D$  indicate the constants,  $b$  denotes the constant recognized as the stretching rate,  $l$  the

characteristic length,  $T_w$  signifies the wall temperature and  $T_\infty$  represents the constant temperature far away from the sheet.

The dimensionless parameter are;

$$u = bx f_\eta(\eta), v = -\sqrt{by} f(\eta), \text{ Where } \eta = \sqrt{\frac{b}{\gamma}} y \theta(\eta)$$

$$= \frac{T - T_\infty}{T_w - T_\infty}, \text{ where } T_w - T_\infty$$

$$= A \left(\frac{x}{l}\right)^2 \text{ PSTCase}$$

$$= D \left(\frac{x}{l}\right)^2 \text{ PHFCase}$$

(6)

where subscript  $\eta$  denotes derivative w.r.t.  $\eta$ .  $U$  &  $v$  gratify (1). Substituting (6) in (2) and (3)

$$f''' - M^2 f' - (f')^2 + f'' + \beta(2ff'f'' - ff''') + k_2 f' = 0, \quad (7)$$

$$Pr[2f'\theta - \theta'f] = \theta'' + Ec Pr f''^2 + (A^* f' + B^* \theta), \quad (8)$$

$$Pr[2f'g - g'f] = g'' + Ec Pr f''^2 + (A^* f' + B^* g), \quad (9)$$

Equation (5)'s boundary conditions change to

#### PST CASE

$$f_\eta(\eta) = 1, \theta(\eta) = 1, f(\eta) = 0 \text{ at } \eta = 0$$

$$f_\eta(\eta) \rightarrow 0, \theta(\eta) \rightarrow 0, f_{\eta\eta}(\eta) \rightarrow 0 \text{ as } \eta \rightarrow \infty$$

(10)

#### PHF CASE

$$f_\eta(\eta) = 1, \theta_\eta(\eta) = -1, f(\eta) = 0 \text{ at } \eta = 0$$

$$f_\eta(\eta) \rightarrow 0, \theta(\eta) \rightarrow 0, f_{\eta\eta}(\eta) \rightarrow 0 \text{ as } \eta \rightarrow \infty$$

(11)

$\beta$  denotes the elastic parameter,

$k_2$  represents “the porosity parameter,

$M$ - presents the magnetic parameter,

$Pr$ -signifies the Prandtl number,

$Ec$ - indicates the Eckert number,

$A^*$ - denotes the space temperature-dependent heat source/sink

$B^*$ -presents the temperature-dependent heat source/sink”.

$\tau_w$  –signifies the shear stress

$Nu$ - denotes the Nussult number. These quantities are,

$$k_2 = \frac{\gamma}{bk'}, M^2 = \frac{\sigma B_0^2}{b\rho}, \quad Pr = \frac{\mu C_p}{K_\infty}, \quad Ec = \frac{b^2 l^2}{Ac_p}$$

$$\tau_w = \frac{\tau^*}{\mu b x \sqrt{b/\gamma}} = f_{\eta\eta}(0), \text{ Where } \tau^* = -\mu \left(\frac{\partial u}{\partial y}\right)_{y=0}$$

(12)

$$Nu = \frac{-h}{T_w - T_\infty} T_w = \left\{ \begin{array}{l} \theta_\eta(0) \text{ PSTCase} \\ 1/\theta(0) \text{ PHFCase} \end{array} \right\}$$

(13)

### 3 Numerical Solution

We utilize the highly efficient shooting technique, as detailed in references De Boor and Conte [21] and Bradshaw and Cebeci [22], in conjunction with a 4th-order Runge-Kutta integration method to address the boundary value issues discussed earlier in the preceding section. In the PST and PHF scenarios, we convert the nonlinear equations (14) and (15) into five first-order ODEs.

$$\frac{df_0}{d\eta} = f_1,$$

$$\frac{df_1}{d\eta} = f_2,$$

$$\frac{df_2}{d\eta} = \frac{(f_1)^2 + M^2 f_1 - f_0 f_2 - 2\beta f_0 f_1 f_2 - k_2 f'}{1 - \beta f_0^2}, \quad (14)$$

$$\frac{d\theta_0}{d\eta} = \theta_1,$$

$$\frac{d\theta_1}{d\eta} = Pr[2f_1\theta_0 - \theta_1 f_0] - Ec Pr f_2^2 + (A^* f' + B^* \theta).$$

The boundary conditions (9) then take the form,

$$f_0(0) = 0, f_1(0) = 1, f_1(\infty) = 0,$$

$$f_2(0) = 0, \theta_0(0) = 0, \theta_0(\infty) = 0.$$

(15)

Here  $f_0 = f(\eta)$  and  $\theta_0 = \theta(\eta)$ . First finding the missing slopes  $f_2(0)$  and  $\theta_1(0)$  by shooting technique. The convergence criteria significantly depend on estimations of the firing procedure's initial conditions that are deemed to be fairly reliable. The iterative operation will continue until the relative variation between the most recent iterative values of  $f_2(0)$  and the most prior iterative value of  $f_2(0)$  are equal, with a tolerance of  $10^{-6}$ . To get the crucial outcome, integrate the resulting ODE using the 4th-order Runge-Kutta technique after attaining convergence.

### 4 Results and Discussion

The results of numerical computations for different physical parameters are shown visually in Figures 1 - 11. The 4th order Runge-Kutta with shot technique approach was used to solve the nonlinear ODEs (7 to 9) subject to boundary conditions (5), (9), and (10) numerically. Visual representations and a brief description of the impact of various parameters on the velocity and temperature profiles are provided.

Figures 1 & 2 depict a variation of  $M$  with  $\beta = 1$  on the velocity profile. A rise in the  $M$  corresponds to a reduction of the velocity profile along  $u$  and  $v$ . The applied transverse magnetic field creates Lorentz force drag, which reduces velocity. Figures 3 and 4 depict the variation of  $\beta$  with  $M = 1$  on the velocity profile. A rise in  $\beta$  is observed to decline the velocity profile along  $u$  &  $v$ . Figs. 5 and 6 reveal that, the effect of  $\gamma$  with  $M = \beta = 1$  on the velocity profile. A rise in  $\gamma$  corresponds to a rise in velocity profile along  $u$  and  $v$ .

Fig. 7(a) & 7(b) reveal “the effect of  $Pr$  on the profiles of temperature for 2 special cases PST and PHF. As  $Pr$  increases the temperature increases monotonously from  $T_s$  to  $T_0$ . The thermal boundary layer thickness drops significantly For high values of  $Pr$ , or low thermal diffusivity.

Figures 8(a) and 8(b) depict the impact of  $Ec$  on the temperature profiles for two unique instances, PHF and PST.  $Ec$  has the power to raise the fluid's temperature. Higher  $Ec$  values, then, suggest a thickening of the thermal boundary layer. Figs. 9(a) and 9(b) show the impact of the space-dependent parameter,  $A^*$ , on the

temperature profiles for two unique situations, PHF and PST. In the PST and PHF cases, the thermal boundary layer generates energy that causes the temperature to increase in magnitude with raising values of,  $A^* (> 0)$  whereas for,  $A^* (< 0)$  The boundary layer fascinates energy that causes the temperature to significantly decrease with reducing values of  $|A^*|$ . For some negative values of  $A^*$ , it is seen in all these plots that there is a heat transfer from the boundary layer area to the sheet.

Figures 10(a) and 10(b) for the PHF and PST instances illustrate how the temperature-dependent parameter,  $B^*$ , affects heat transport. According to these graphs, energy is released for rising values of  $B^* (> 0)$  which results in temperature increases in PST and PHF situations, but energy is absorbed for falling values of  $B^* (< 0)$  which causes the temperature to fall sharply close to the boundary layer.

Figures 11(a and b) shows that, the effect of porosity  $\gamma$  with  $M = \beta = 1$  on the temperature profile. When the porosity parameter is raised, the temperature falls in the PST case, while the converse is true in the PHF case.

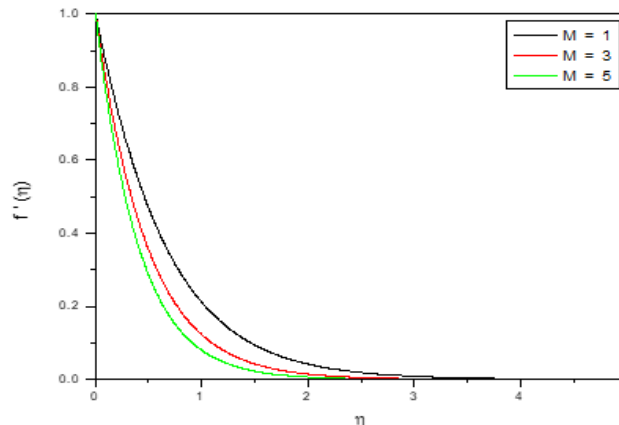


Fig. 1 The effect of MHD parameter  $M$  on  $u$ -velocity component  $f'$  at  $\beta = 1$

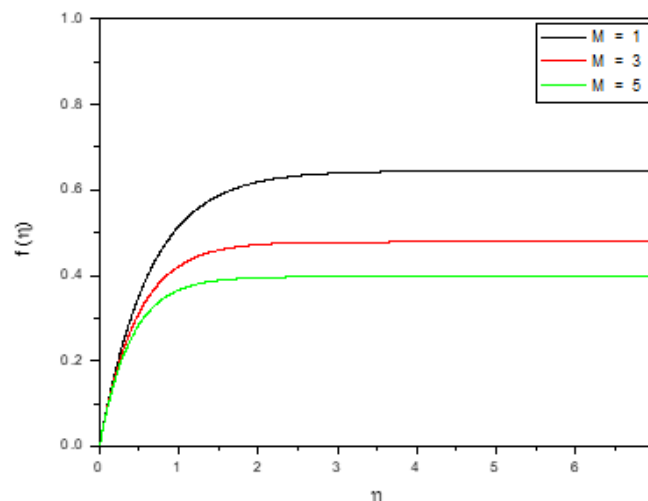


Fig. 2. The effect of MHD parameter  $M$  on  $v$ -velocity component  $f$  at  $\beta = 1$

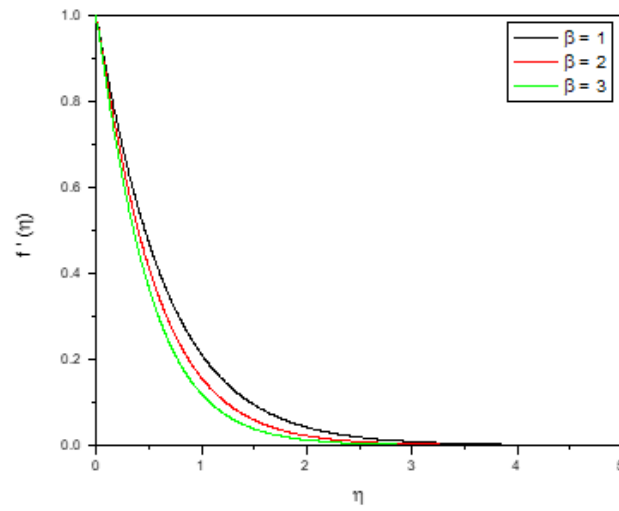


Fig. 3. The effect of elastic parameter  $\beta$  on  $u$ -velocity component  $f'$  at  $\beta=1$

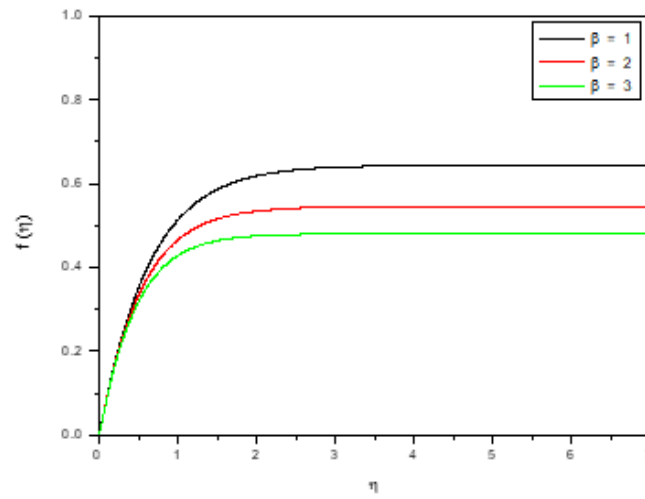


Fig. 4. The effect of elastic parameter  $\beta$  on  $V$ -velocity component  $f$  at  $\beta = 1$

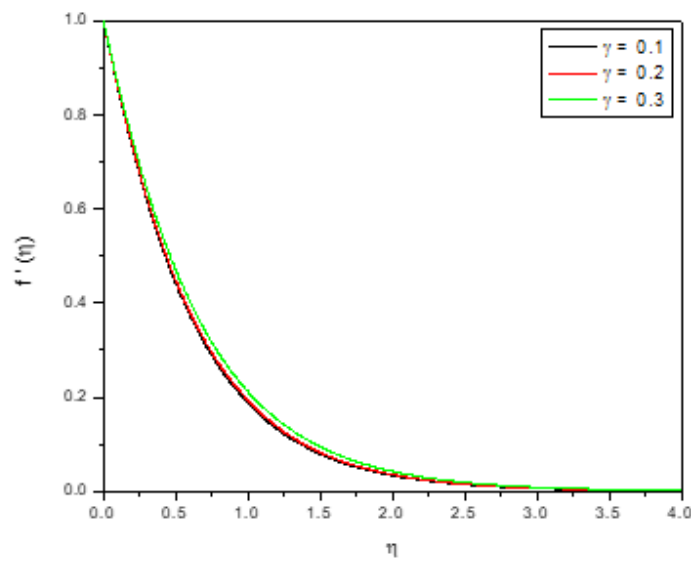


Fig. 5 The effect of Porous parameter  $\gamma$  on  $u$ -velocity component  $f'$  at  $M=\beta=1$

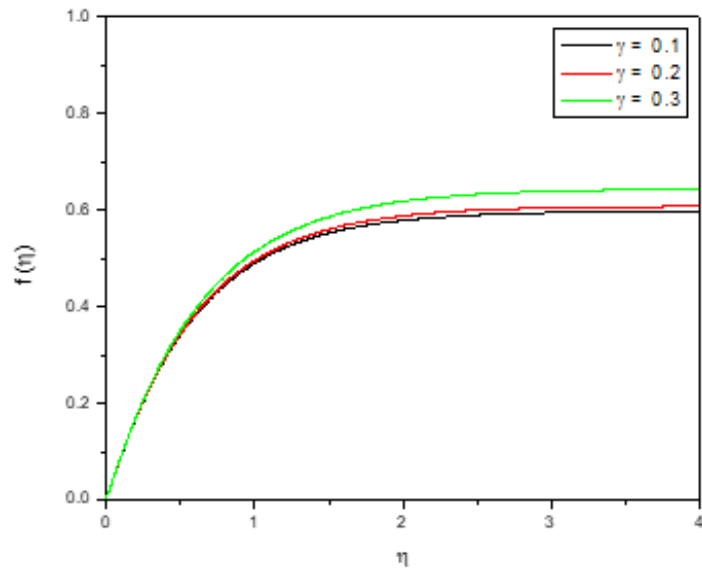


Fig. 6. The effect of Porous parameter  $\gamma$  on v-velocity component  $f$  at  $M=\beta=1$

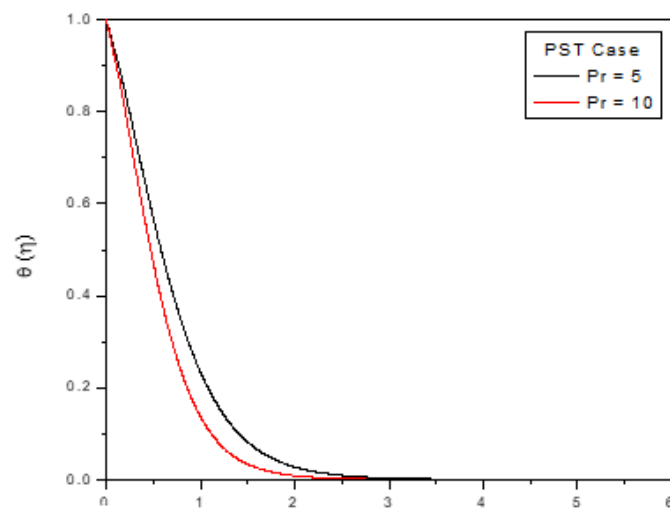


Fig. 7a. The effect of Prandtl number Vs Temperature profile

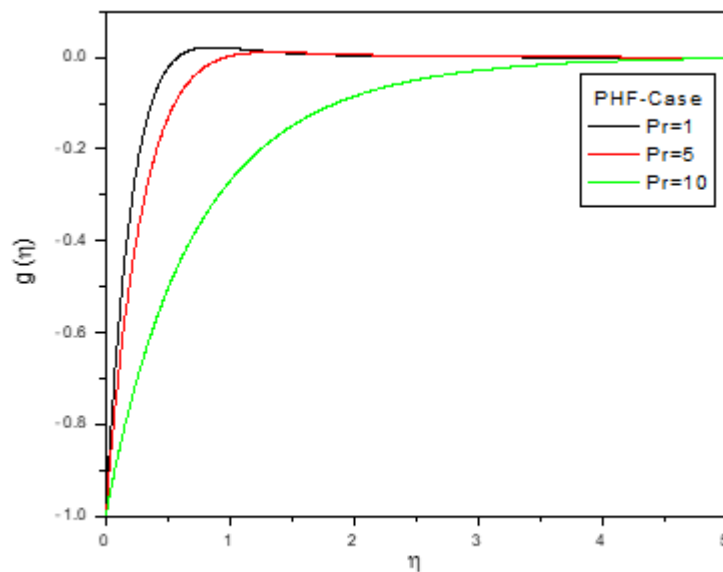


Fig. 7b. The effect of Prandtl number Vs temperature profile

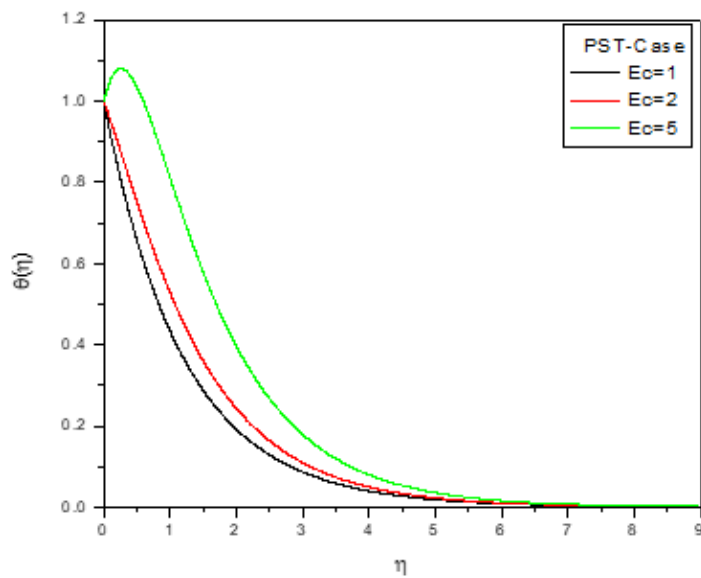


Fig. 8a. The effect of Eckert number Vs temperature profile

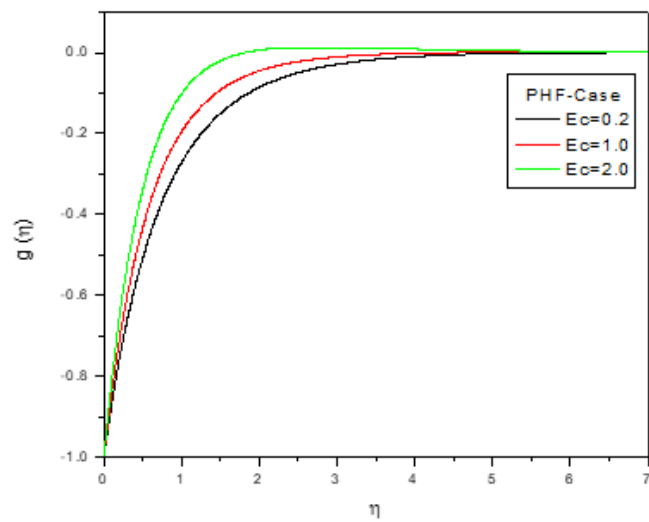


Fig. 8b. The effect of Eckert number Vs Temperature profile

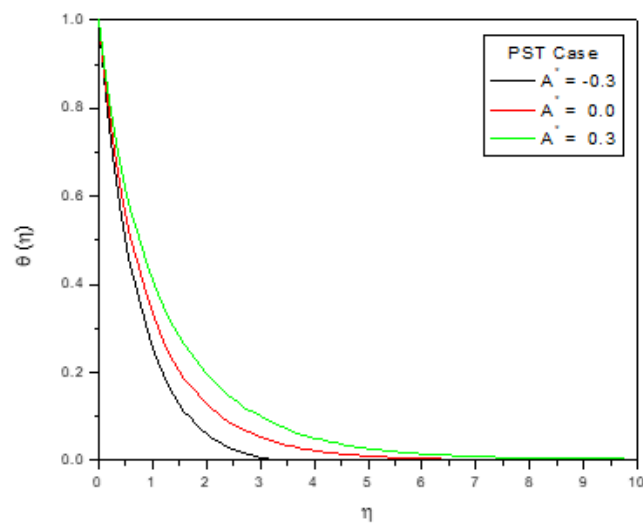


Fig. 9a. The effect of nonuniform heat source Vs Temperature profile

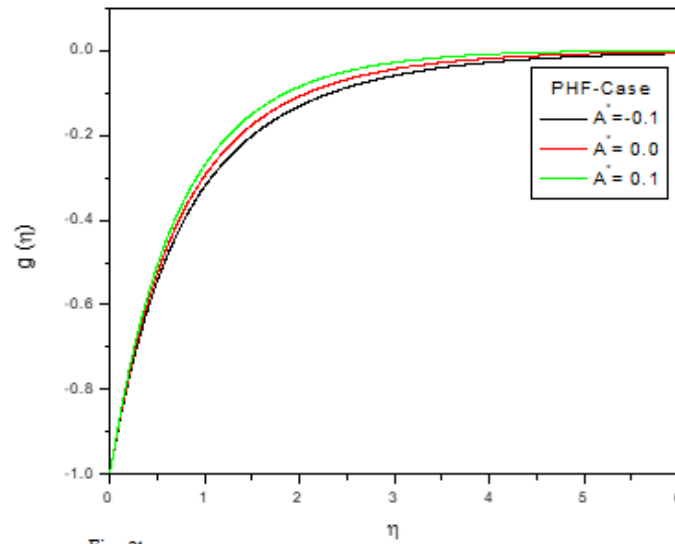


Fig. 9b. The effect of nonuniform heat source Vs temperature profile

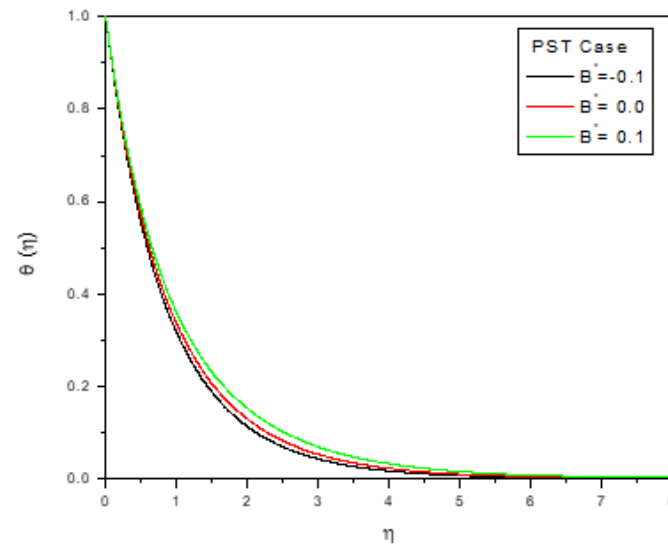


Fig. 10a. The effect of nonuniform heat sink Vs Temperature profile

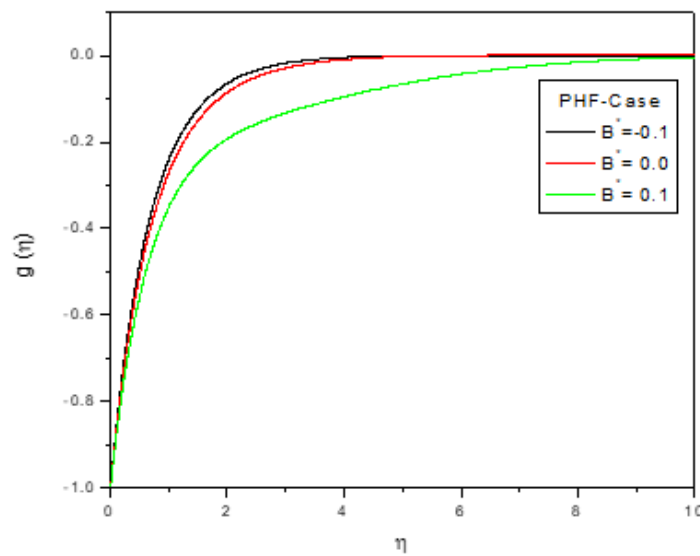


Fig. 10b. The effect of nonuniform heat sink Vs Temperature profile



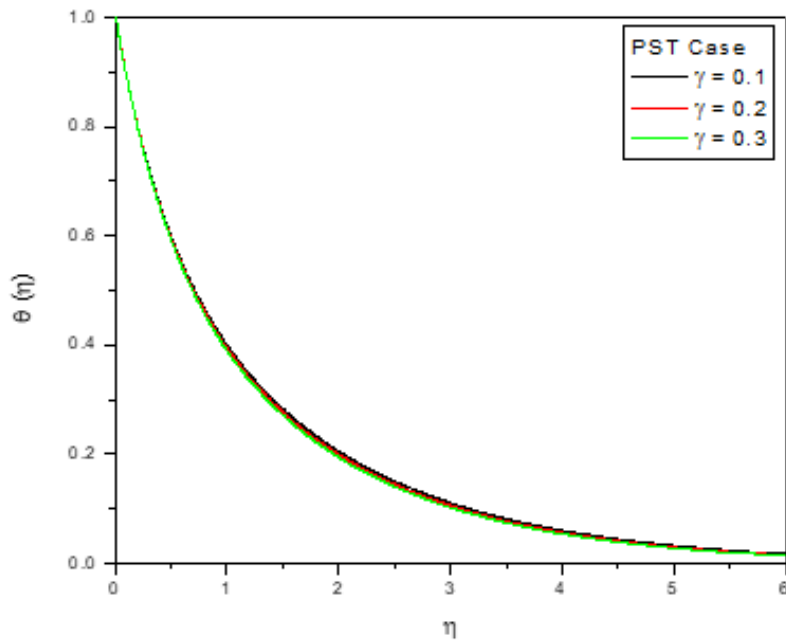


Fig. 11a. Effect of porous parameter  $\gamma$  on temperature profile in PST Case

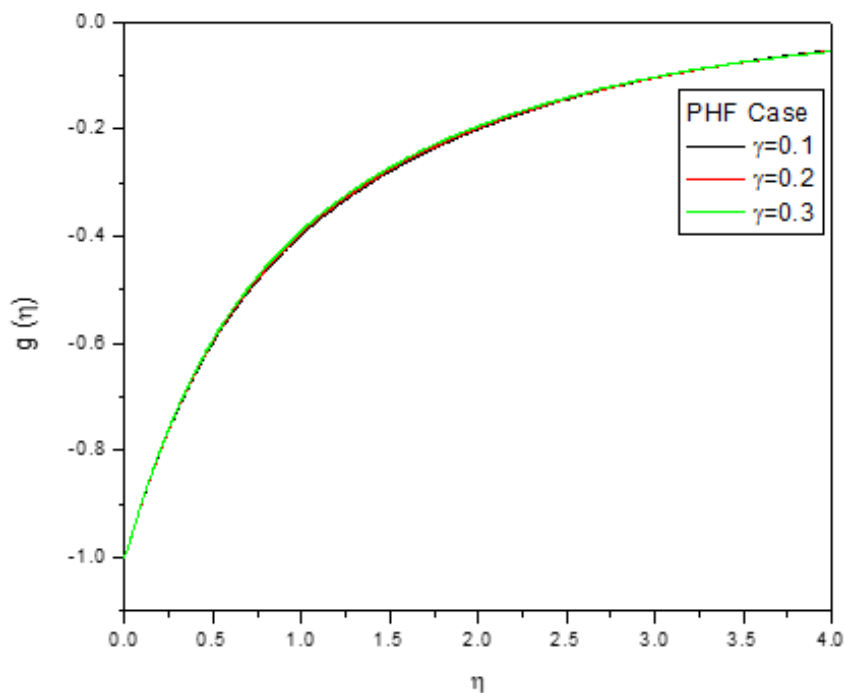


Fig. 11b. Effect of Porous parameter  $\gamma$  on temperature profile in PHF Case

## 5 Conclusions

1. In a viscous, incompressible, electrically conducting fluid, the existence of a transverse magnetic field causes the velocity field to decrease, leading to a rise in the temperature field.

2. Eckert number measures viscosity. In the incidence of viscous dissipation, dimensionless temperature increases with fluid heating ( $Ec > 0$ ) and decreases with cooling ( $Ec < 0$ ). Viscous dissipation raises thermal boundary layer temperature.

3. The temperature rises for positive values of the heat source/sink parameters and falls for negative values. Therefore, non-uniform heat sinks are preferable for cooling purposes.

## Nomenclature:

$C_f$	skin friction coefficient
$f$	dimensionless stream function
$h$	dimensionless concentration function

$k$	thermal conductivity
$M$	magnetic parameter
$Nu_x$	local Nusselt number
$Pr$	Prandtl number
$Re_x$	local Reynolds number
$T$	temperature of the fluid inside the boundary layer
$T_w$	temperature at the surface of the sheet
$T_\infty$	ambient temperature
$U_\infty$	free stream velocity
$u, v$	velocity component along x- and y-direction

### Greek symbols

$\eta$	dimensionless similarity variable
$\mu$	dynamic viscosity of the fluid
$\nu$	kinematic viscosity of the fluid
$\psi$	stream function
$\alpha$	thermal diffusivity
$\sigma$	electrical conductivity
$\Theta$	dimensionless temperature
$\infty$	condition at the free stream
$W$	condition at the surface

### References:

- [1] L.J. Crane, flow past a stretching plate, *Z. Angew. Math. Phys.* 21 (1970) 645-647.
- [2] J.B. McLeod, K.R. Rajagopal, On the uniqueness of flow of a Navier-Stokes fluid due to a stretching boundary, *Arch. Rational Mech. Anal.* 98 (1987) 699-709
- [3] W.C. Troy, W.A. Overman II, G.B. Ermentrout, Uniqueness of flow of a second-order fluid past a stretching sheet, *Quart. Appl. Math.* 45 (1987) 753-755.
- [4] P.S. Gupta, A.S. Gupta, Heat and Mass Transfer on a stretching sheet with suction or blowing, *Can. J. Chem. Engng.* 55 (1977) 744-746.
- [5] Char, Ming-I. "Heat transfer of a continuous, stretching surface with suction or blowing." *Journal of mathematical analysis and applications* 135, no. 2 (1988): 568-580.
- [6] L.G. Grubka, K.M. Bobba, Heat Transfer characteristics of a continuous stretching surface with variable temperature, *J. Heat Transfer* 107 (1985) 248-250.
- [7] T.C. Chiam, Magnetohydrodynamic heat transfer over a non-isothermal stretching sheet, *Acta Mechanica* 122 (1997) 169-179.
- [8] K. Vajravelu, D. Rollins, Heat transfer in electrically conducting fluid over a stretching surface, *Int. J. Non-Linear Mech.* 27 (2) (1992) 265-277.
- [9] Emad M. Abo-Eldahab, Mohamed A. El Aziz, Blowing/Suction effect on hydromagnetic heat transfer by mixed convection from an inclined continuously stretching surface with internal heat generation/absorption, *Int. J. Therm. Sci.* 43 (2004) 709-719.
- [10] Abbas, Z., M. Sajid, and T. Hayat. "MHD boundary-layer flow of an upper-convected Maxwell fluid in a porous channel." *Theoretical and Computational Fluid Dynamics* 20 (2006): 229-238
- [11] Hayat, Tasawar, Niaz Ali, and Saleem Asghar. "Hall effects on peristaltic flow of a Maxwell fluid in a porous medium." *Physics Letters A* 363, no. 5-6 (2007): 397-403.
- [12] Sadeghy, Kayvan, Amir-Hosain Najafi, and Meghdad Saffaripour. "Sakiadis flow of an upper-convected Maxwell fluid." *International Journal of Non-Linear Mechanics* 40, no. 9 (2005): 1220-1228.
- [13] Hayat, T., Z. Abbas, and M. Sajid. "Series solution for the upper-convected Maxwell fluid over a porous stretching plate." *Physics Letters A* 358, no. 5-6 (2006): 396-403.
- [14] Sadeghy, Kayvan, Hadi Hajibeygi, and Seyed-Mohammad Taghavi. "Stagnation-point flow of upper-convected Maxwell fluids." *International journal of non-linear mechanics* 41, no. 10 (2006): 1242-1247.
- [15] Aliakbar, V., A. Alizadeh-Pahlavan, and K. Sadeghy. "The influence of thermal radiation on MHD flow of Maxwellian fluids above stretching sheets." *Communications in Nonlinear Science and Numerical Simulation* 14, no. 3 (2009): 779-794.
- [16] Renardy, Michael. "High Weissenberg number boundary layers for the upper convected Maxwell fluid." *Journal of Non-Newtonian Fluid Mechanics* 68, no. 1 (1997): 125-132.
- [17] Rao, I. J., and K. R. Rajagopal. "On a new interpretation of the classical Maxwell model." *Mechanics Research Communications* 34, no. 7-8 (2007): 509-514.
- [18] Alizadeh-Pahlavan, Amir, and Kayvan Sadeghy. "On the use of homotopy analysis method for solving unsteady MHD flow of Maxwellian fluids above impulsively stretching sheets." *Communications in Nonlinear Science and Numerical Simulation* 14, no. 4 (2009): 1355-1365.
- [19] Aliakbar, V., Alizadeh-Pahlavan, A., & Sadeghy, K. (2009). The influence of thermal radiation on MHD flow of Maxwellian fluids above stretching

sheets. *Communications in Nonlinear Science and Numerical Simulation*, 14(3), 779-794.

- [20] Alizadeh-Pahlavan, Amir, Vahid Aliakbar, Farzad Vakili-Farahani, and Kayvan Sadeghy. "MHD flows of UCM fluids above porous stretching sheets using two-auxiliary-parameter homotopy analysis method." *Communications in Nonlinear Science and Numerical Simulation* 14, no. 2 (2009): 473-488.
- [21] Conte, S. D., and Carl de Boor. "Numerical Analysis: An Algorithmic Approach." (1972).
- [22] Cebeci, Tuncer, Peter Bradshaw, Tuncer Cebeci, and Peter Bradshaw. "Conservation Equations for Mass, Momentum, and Energy." *Physical and Computational Aspects of Convective Heat Transfer* (1984): 19-40.